JOURNAL OF GUIDANCE, CONTROL, AND DYNAMICS
Vol. 27, No. 1, January–February 2004

Rule-Based Cooperative Control of Optically Linked Model Spacecraft: Experimental Study

P. K. C. Wang,* J. Yee,† and E. G. Sayegh†
University of California, Los Angeles, Los Angeles, California 90095-1594
and
F. Y. Hadaegh‡
Jet Propulsion Laboratory, California Institute of Technology, Pasadena, California 91109-8099

An experimental study is made on the alignment of an optically linked autonomous model-spacecraft triad with features similar to those in a separated-spacecraft interferometer. Each model spacecraft is magnetically levitated and free to rotate about a fixed axis. Two laser beams are used to simulate the light from a distant star impinging on the collectors of a space interferometer. The laser beams reflected from the servo-controlled mirrors on the collector model spacecraft impinge on an optical sensor array mounted on the combiner model spacecraft. Simple rule-based cooperative controls are developed for optical alignment in the presence of rotational drift induced by external impulsive or persistent disturbances. These controls are driven by events defined by the laser-beam activation of certain sensors. The resulting controlled system is a hybrid continuous-time and discrete-event system. Experimental results show that the derived control laws are effective in achieving optical alignment of the model spacecraft triad, using only a small number of optical sensors with binary outputs, provided that the relative angular drift speeds are sufficiently small.

Introduction

THE feasibility of using long flexible booms in space interferometers has been studied both analytically and experimentally.[1–3] Because of boom vibrations, there is a practical limit on the boom length, which in turn sets a limit on the length of the baseline. To overcome this limitation and to provide flexibility of operation, the use of multiple free-flying spacecraft for a long-baseline space interferometer has been proposed.[4–7] Figure 1 shows a typical configuration involving three spacecraft placed at the vertices of an equilateral triangle. The starlight impinges on the mirrors attached to two spacecraft, called the collectors, and then reflects toward the optical sensor of the third spacecraft, called the combiner. In the operation of the interferometer, the initial task is to configure the spacecraft in a triangular pattern with specified separation distances. The subsequent task is to orient each spacecraft so that the reflected light from the collector impinges on the combiner's optical sensor with a position accuracy in the sensor plane on the order of a fraction of the optical wavelength. To reconstruct the target image, it is necessary to gather interferometry data for various formation orientations by slewing the spacecraft formation from one orientation to another while maintaining the triangular formation pattern. Because of the limited aperture of the optical elements and the stringent pointing accuracy requirements, it is necessary to use multimode controllers. A typical approach is to use a dual-mode controller with coarse and fine modes. In the coarse mode, the triangular spacecraft formation pattern is attained by activating the appropriate thrusters. Then the attitudes of the collectors are slewed to capture the starlight. Finally, the mirrors of the collectors are rotated so that the reflected light impinges on the sensor of the combiner. Once this task is accomplished, it is necessary to maintain starlight capture in the presence of any external and internal disturbances. For a space interferometer with collectors and combiner attached to a flexible boom, a basic control problem is to isolate the optical elements from disturbances induced by boom vibrations. In the case of a space interferometer with free-flying collectors and combiner, the control system for optical alignment must function with augmented degrees of freedom. Most likely, minute disturbances such as those due to micrometeorite impact could induce slow drift of the spacecraft relative attitude and position. When the fine-mode control is unable to compensate for the drift, switching to the coarse mode may result in overcompensation and undesirable mode cycling, which lead to excessive fuel consumption. To the best of our knowledge, no in-flight or laboratory experimental studies have been made on the effect of controller mode switching induced by relative attitude and separation drift on the system's optical performance. Recently, the optical link between the French SPOT-4 satellite and the European Space Agency's ARTEMIS telecommunication satellite via laser beams was successfully demonstrated.[8] Although the space interferometer's pointing accuracy requirement for optical alignment is more stringent than that of the aforementioned satellites, the European experiment represents a significant step toward implementing multiple optically linked spacecraft in precise formations.

Here, in the spirit of our earlier experimental studies,[9–10] the main objective is to develop cooperative rule-based controls for multiple autonomous model spacecraft (MS) performing the aforementioned tasks, taking into consideration the relative-attitude drift of the MS induced by impulsive or persistent disturbances. The controls are cooperative in the sense that communication of relevant data between the MS is used to generate the appropriate control actions such as in the case of multiple robots performing a common task. The control actions are based on rules determined by the occurrence and time duration of certain discrete-event sequences defined by the activation of certain optical sensors with binary outputs by the incoming light beams. The main advantages of these controls are as follows:

1) Precise measurement of the system variables is unnecessary; therefore low-cost sensors and actuators can be used in the implementation of controllers.

2) Control rules can be developed using binary sensor data directly without extensive processing and system dynamic models.

3) Control rules are in the form of logical statements that can be easily programmed.

Because the optical sensor outputs are binary-valued, the alignment accuracy attainable by such a control system depends primarily on

Received 1 October 2002; revision received 15 July 2003; accepted for publication 31 July 2003.

*Professor, Department of Electrical Engineering. Member AIAA.
†Graduate Student, Department of Electrical Engineering.
‡Senior Research Scientist and Technical Supervisor, Guidance and Control Analysis. Associate Fellow AIAA.

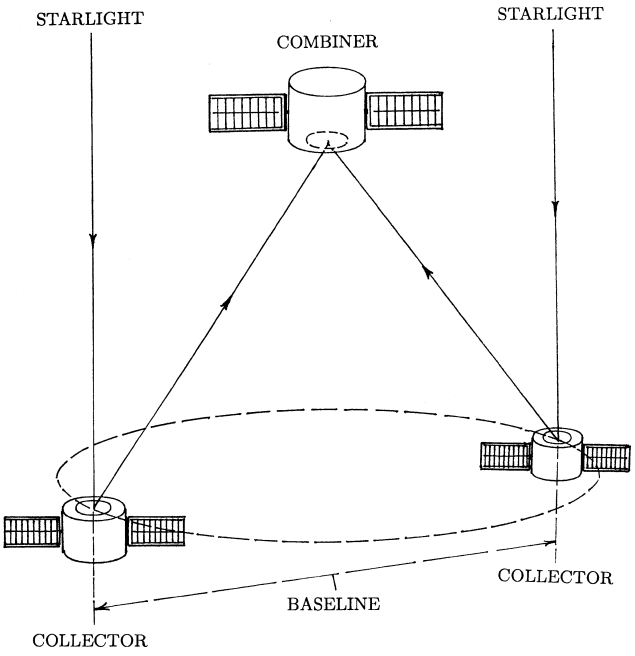

Fig. 1 Sketch of spacecraft triad in a triangular formation for space interferometry.

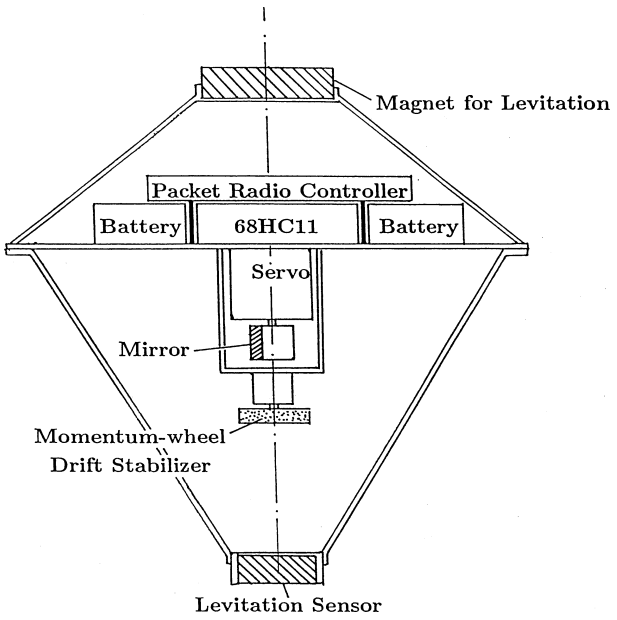

Fig. 2 Sketch of collector model spacecraft.

the geometric dimensions of the sensors and the incoming light beams. The main disadvantage of these controls is that they lead to hybrid systems whose dynamical behavior cannot be easily analyzed. Therefore, we resort to an experimental study of the effectiveness of the developed rule-based controls using a magnetically levitated model-spacecraft triad in a laboratory environment. Because it is extremely difficult to design magnetic-levitation systems for levitating objects with full degrees of freedom, we restrict ourselves only to magnetically levitated MS that are free to rotate about a single fixed axis. In what follows, a description of the experimental setup is given first. Then, rule-based cooperative controls are developed. Following that, the results for a typical experiment are presented. The paper concludes with a discussion of the experimental results.

Experimental Setup

To simulate the microgravity space environment, three model autonomous spacecraft are levitated magnetically. Because the equilibria of objects levitated by static magnetic fields are generally unstable, it is necessary to use feedback controls for stabilization. Here each MS is equipped with a permanent magnet mounted on top of its aluminum frame (see the sketch of a collector MS shown in Fig. 2). The levitation force is generated by the interaction of the permanent magnet with an electromagnet driven by a pulse-width modulated power transistor circuit. A small permanent magnet attached to the bottom of the aluminum frame provides a nearly vertical magnetic field to interact with the sensor consisting of a multiturn coil. Any motion of the MS induces a voltage across the stationary sensor coil. This signal is fed back to the electromagnet driver. In our experimental setup, the levitation system is capable of levitating a 1-kg MS without experiencing significant instability problems. Moreover, the system is robust with respect to external disturbances. Because our emphasis here is placed on optical alignment, the details for the levitation control system are not given. In our earlier experimental study,[9] where three autonomous MS were levitated by pressurized air bearings formed by the flat bottom surface of their bodies and a flat granite surface, each MS was equipped with a laser beam and optical sensor for seeking out the remaining MS to achieve a triangular formation pattern. No optical alignment with respect to external light sources was attempted. Here, external stationary 3-mW laser beams are used to simulate the starlight sources. These beams are used directly in the optical alignment of the MS. Thus, the basic elements in this experimental setup resemble those in an

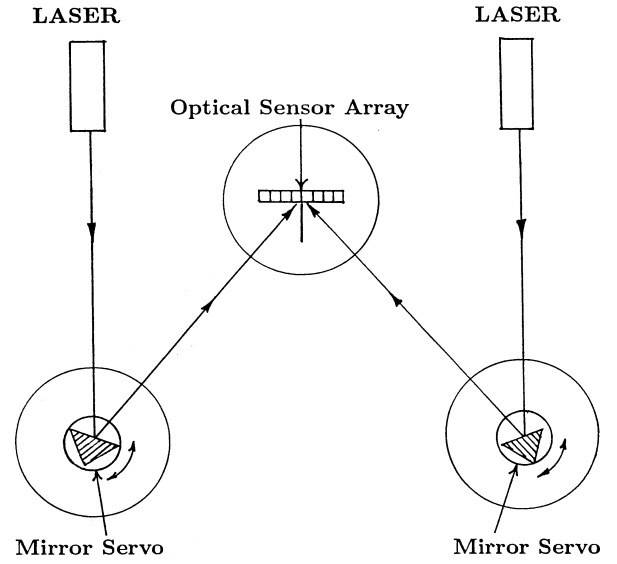

Fig. 3 Sketch of laboratory model spacecraft triad in a triangular formation.

actual space interferometer (see Fig. 3 for a sketch). A photograph of the actual experimental setup is shown in Fig. 4. In what follows, we give a more detailed description of the experimental setup.

Collector and Combiner

In our experiment, the levitated collector and combiner MS (referred to simply as "collector" and "combiner" hereafter) are placed at the vertices of an equilateral triangle with 0.745-m sides. The central part of the collector is a high-quality mirror mounted on a servo-driven platform (see Fig. 5). The combiner's sensor array is displaced from the triangle's vertex such that each side of the equilateral triangle formed by the centers of the mirrors and sensor array has a length $l = 0.68$ m. To determine the minimum movement of the servo to achieve a specified shift of the incoming laser beam, let the mirror be rotated with an angle θ about the axis centered at the impact point of the laser beam (see Fig. 6). Assuming that the cross section of the laser beam has zero diameter, it can be verified by simple geometry that the rotational angle θ is related to the shift D at the point of impact of the laser beam on the sensor-array

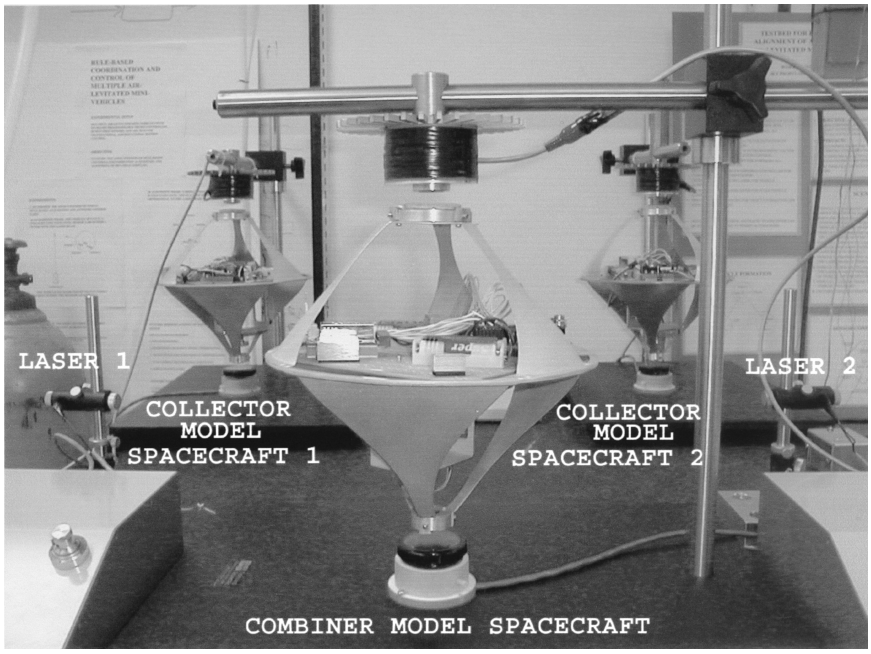

Fig. 4 Photograph of actual experimental setup.

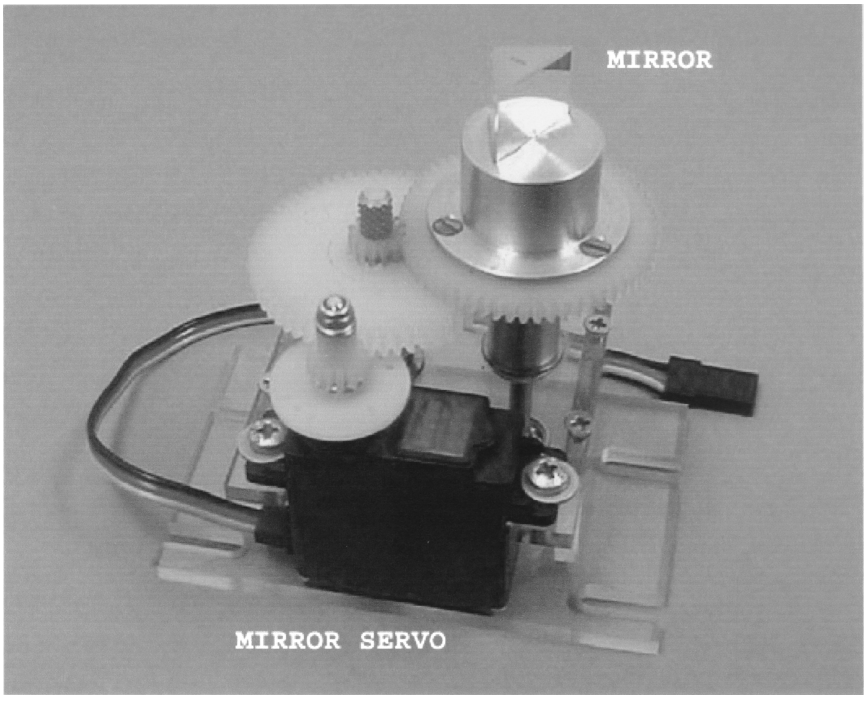

Fig. 5 Photograph of mirror servo platform.

plane by

$$\theta = \frac{1}{2}\cos^{-1}\left(\frac{2l + D}{2\sqrt{l^2 + lD + D^2}}\right) \tag{1}$$

In our combiner, the width of each sensor element in the array is 0.002 m, and the equilateral triangle's side has length $l = 0.68$ m. Setting D equal to the sensor width, we obtain from Eq. (1) that $\theta = 0.0728$ deg. Evidently, a minute rotation of the mirror will induce a large deflection of the intersection point of the reflected beam with the sensor-array plane at a distance of 0.68 m. The effective gain between the beam displacement and mirror rotation is 27.47 mm/deg. Therefore, a reduction gear between the servomotor shaft and the mirror platform is needed to limit the mirror rotation to a useful range. To determine a suitable gear ratio, a test with the mirror driven directly by the servo was performed. It was noted that the smallest movement that could be reliably made by the servo was about 10 times the diameter of the laser beam. Because the width of each sensor element was approximately twice the laser beam diameter, a 10-to-1 gear ratio was selected. Although a 20-to-1 gear ratio may have the potential of centering the laser beam on the sensor array more precisely, the magnitude of gear dead zone and backlash along with the servo speed limitation seem to preclude that possibility.

The mirror servo for the collectors is a pulse-width modulated feedback control system. The zero angular position of the servo output corresponds to a symmetric positive 60-Hz square pulse train applied to the servo input command. Clockwise or counterclockwise

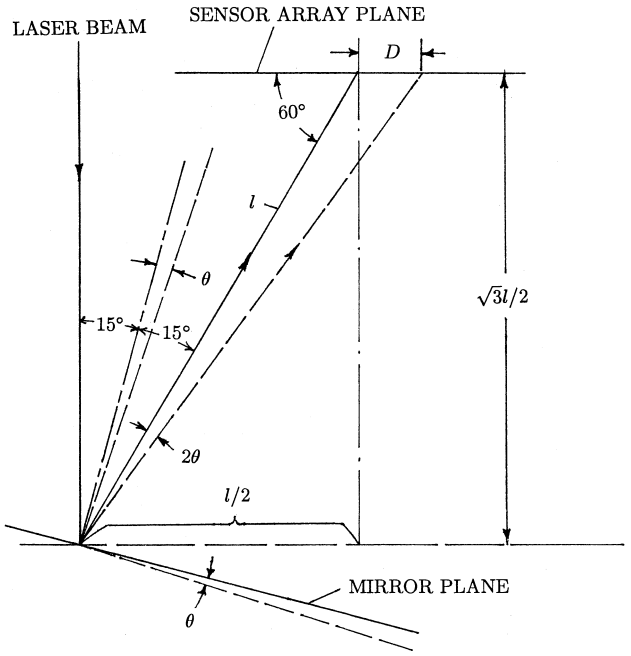

Fig. 6 Geometry of laser beam in the presence of mirror rotation.

servo-output stepping motion is produced by increasing or decreasing the duration of the positive pulse in discrete time steps. The maximum angular excursion of the mirror servo output is approximately 135 deg. The geared-down servo angular resolution is approximately 0.188 deg.

The rotational motions of the left (L) and right (R) collectors about their vertical axes are describable by

$$I_i \frac{\mathrm{d}^2\theta_i}{\mathrm{d}t^2} + \nu_i \frac{\mathrm{d}\theta_i}{\mathrm{d}t} = \tau_{ic} + \tau_{id}, \qquad i = L, R \tag{2}$$

where I_i, ν_i, and θ_i are the moment of inertia, friction coefficient, and the angular position of the ith collector about a given inertial reference frame, respectively. With zero control torque τ_{ic}, the collectors may exhibit small motions induced by nonzero initial conditions and/or impulsive and persistent disturbance torque τ_{id}.

The basic element of the combiner is an optical sensor array for sensing the laser beams reflected from the mirrors of the collectors. Because of the limited number of inputs to the microcontroller, the array is made up of only eight sensors. The actual layout of the sensor array can be seen from the photograph of the combiner shown in Fig. 7. An opaque light shield is introduced at the center of the sensor array so that the left (and respectively right) four sensors can be activated only by the laser beam from the left (and respectively right) collector. One of the sensors in the left or right sensor array is designated as the target sensor for the corresponding reflected laser beams.

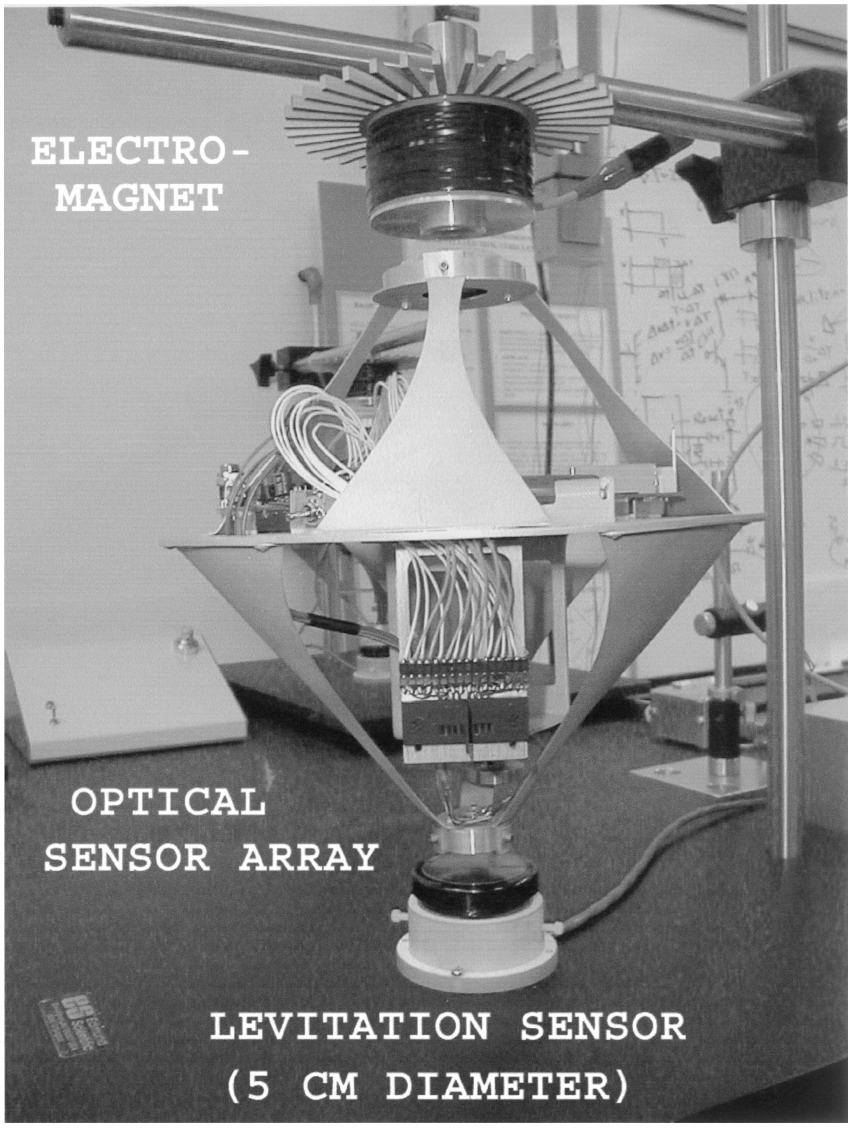

Fig. 7 Close-up photograph of combiner model spacecraft showing the sensor array.

For our experimental setup, three modes of control for optical alignment are proposed, namely, the coarse, intermediate, and fine modes. The fine mode is activated when the laser beam hits the sensor array. The control objective is to steer the beam to the target sensor. The intermediate mode is activated when the sensor array is first hit by the laser beam, and then the beam exits from the sensor array in the subsequent time step. The control objective is to recapture the beam. Finally, the coarse mode is activated when the laser beam does not hit the sensor array in two successive time steps. The control objective is to search the laser beam by changing the attitude of the entire MS. This task usually requires the introduction of an additional control system for large-attitude maneuvers using the control torque τ_{ic}. In our setup, this mode is implemented by requiring the mirror servo to scan over its entire range of angular displacements when searching for the laser beam.

Data Communication and Telemetry Systems

Each MS is equipped with a UHF 40-kb/s packet radio transceiver for inter-MS data communication and telemetry. The inter-MS data communication permits cooperative control between the combiner and the collectors for optical alignment. The main function of telemetry is to monitor the sensor data from the combiner and the motions of the mirror servos of the collector. Thus, the dynamic behavior of each MS can be recorded for subsequent analysis, and the performance of the overall system can be determined.

Microcontroller

The heart of the cooperative control system for the collector or combiner is a Motorola MC68HC811E2 microcontroller. In the collector, the microcontroller serves both as a command generator for the mirror servo and a decoder for the packet radio signals from the combiner. In the combiner, the main function of the microcontroller is to determine which sensors are being hit by the laser beams and to transmit that information to the collector via the onboard packet radio. Based on this information, the collector's controller executes appropriate corrective action to its mirror servo. Because the microcontroller has only 2 kB of programmable memory, the algorithms for control and sensor signal processing are implemented in assembly language. Because the microcontroller of each MS receives no external commands, the MS are completely autonomous, and they interact with each other via optical and/or radio channels.

Rule-Based Controls

Because the laser beam has nonzero diameter, and the sensor output voltage depends on the beam intensity and the area of the sensor element that is exposed to the laser beam, it is necessary to set suitable thresholds for deciding whether or not the sensor is considered a hit. Thus, the sensor output is binary valued. Let the state of the ith sensor ($i = R, L$) be denoted by the binary-valued variable s_i, where $i = L1, \ldots, L4, R1, \ldots, R4$. Let the states of the left and right sensor arrays be specified by the respective binary strings $\boldsymbol{s}_L = (s_{L4}, s_{L3}, s_{L2}, s_{L1})$ and $\boldsymbol{s}_R = (s_{R1}, s_{R2}, s_{R3}, s_{R4})$ subject to the constraint that the sum of the elements of each string is either 0 or 1 (at most one sensor can be hit by the laser beam). Because, for each $\boldsymbol{s}_L$, the right sensor array could be in any of the five states [i.e., $\boldsymbol{s}_R = (0,0,0,0)$, $(1,0,0,0)$, $(0,1,0,0)$, $(0,0,1,0)$, $(0,0,0,1)$], there are only 25 possible states for the combined left–right sensor array. Assuming that the combiner is stationary and the rotational speed is sufficiently small, then, from a knowledge of $\boldsymbol{s}_L$ and $\boldsymbol{s}_R$ at two different time steps set by the sampling rate of data transmission rate of the packet radio transceiver, we can infer the directions of the rotational motions of the left and right collectors, respectively. In effect, the first-order dynamics of the MS are partially embedded in the sensor data history.

Because the laser beam sweeps across the sensor array in a smooth manner, the sensor state transitions between successive time steps k and $k+1$ are describable by left or right shift operators $\boldsymbol{S}^-$ or $\boldsymbol{S}^+$, respectively; that is, $\boldsymbol{s}_L(k+1) = \boldsymbol{S}^{\pm}\boldsymbol{s}_L(k)$. For example, $\boldsymbol{s}_L(k) = (0, 0, 1, 0)$, $\boldsymbol{S}^+\boldsymbol{s}_L(k) = (0, 0, 0, 1)$, and $\boldsymbol{S}^-\boldsymbol{s}_L(k) = (0, 1, 0, 0)$. Note that $\boldsymbol{S}^+(0, 0, 0, 1) = \boldsymbol{S}^-(1, 0, 0, 0) = (0, 0, 0, 0)$ and $\boldsymbol{S}^{\pm}(0, 0, 0, 0)$ are not defined.

Let the desired states of the left and right sensor arrays of the combiner be specified by $\boldsymbol{s}_L^d = (0, 0, 1, 0)$ and $\boldsymbol{s}_R^d = (0, 1, 0, 0)$, respectively. The main task is to command the mirror servo in each collector so that the corresponding laser beam hits the target sensor specified by the second sensor in the array and locks on to it in the presence of small drift of both the collector and combiner. To derive the control rules for the left and right collectors, we consider all possible discrete events associated with the left and right sensor arrays of the combiner. For the right collector, the events can be classified into the following categories: (c1) $\boldsymbol{s}_R(k) = \boldsymbol{s}_R(k-1) = (0, 0, 0, 0)$, where the right sensor array has no contact with the laser beam; (c2) $\boldsymbol{s}_R(k), \boldsymbol{s}_R(k-1) \neq (0, 0, 0, 0)$, where the right sensor array remains in contact with the laser beam; (c3) $\boldsymbol{s}_R(k-1) \neq (0, 0, 0, 0)$, $\boldsymbol{s}_R(k) = (0, 0, 0, 0)$, where the right sensor array loses contact with the laser beam; and (c4) $\boldsymbol{s}_R(k-1) = (0, 0, 0, 0), \boldsymbol{s}_R(k) \neq (0, 0, 0, 0)$, where the right sensor array gains contact with the laser beam. Similar classification can be made for the left collector.

In the design of the control rules for the collector's mirror servo, we assume that the combiner is stationary. This assumption is justifiable, because in a real space interferometer the combiner will most likely have star trackers and the necessary control hardware to maintain the desired position and attitude. Now, the control-rule design is based on the occurrence of discrete events characterized by the pair of the sensor states at two successive time steps $k-1$ and k. For example, if $\boldsymbol{s}_R(k-1) = (0, 0, 0, 1)$ and $\boldsymbol{s}_R(k) = (0, 0, 0, 0)$, then this pair of sensor states constitutes a discrete event. This event implies that the laser beam from the right collector just walked off the right end of the combiner sensor array under the assumption that the beam movement is sufficiently slow. The discrete events, their inferences, and the control actions for the right collector are tabulated in Table 1. A similar table can be made for the left collector in which $\boldsymbol{s}_L^d = (0, 0, 1, 0)$ is the desired state of the left sensor array.

In Table 1, the rotational motion of the MS is considered to be normal if the laser beam sweeps over not more than one sensor width in one time step so that the mirror servo is able to steer the reflected beam to the target sensor. When the activated sensor element shifts ± 2 sensor widths in one time step, the MS rotational motion is considered to be in the high-velocity regime (Hi-V). If the activated sensor element shifts more than ± 2 sensor widths in one time step, then the MS rotational motion is considered to be abnormal (ABN). We define the admissible control actions (mirror servo commands) to be 0, ± 1, and ± 2 steps, where one step corresponds to the minimum change in servo command that causes the servo to respond. The corresponding mirror angular displacement is approximately 0.188 deg (the geared-down servo angular resolution), which in turn induces a displacement of the reflected laser beam on the sensor array equal approximately to the width of a sensor element.

We assume that the MS rotational motion does not become ABN during a valid experimental run. In event 4, $\boldsymbol{s}_R(k-1) = (0, 0, 0, 0)$ and $\boldsymbol{s}_R(k) = (0, 0, 1, 0)$. These sensor states can be attained by having the reflected laser beam entering from either the right or the left side of the sensor array with 2 or >2 sensor-width movements, respectively, in one time step. In a valid experimental run, the second possibility is ruled out. Thus, we infer that the reflected laser beam enters from the right side of the sensor array with Hi-V. Another possible option is to store both $\boldsymbol{s}_R(k-1)$ and $\boldsymbol{s}_R(k)$ and wait for the sensor state $\boldsymbol{s}_R(k+1)$ at the next time step so that the direction of beam motion can be inferred from the triplet of sensor states. Then a possible special control action is taken by stepping in the direction opposite that of the inferred beam motion. In event 10, $\boldsymbol{s}_R(k-1) = (1, 0, 0, 0)$ and $\boldsymbol{s}_R(k) = (0, 0, 0, 1)$. The reflected laser beam first hits sensor RS1 and then RS4 in the next time step, implying that a left-to-right shift of three sensor widths takes place in one time step. Thus, the MS rotational motion is ABN. In this case, we set the control action to the maximum admissible left shift of two steps. A similar situation occurs in event 22.

The set of control actions or rules can be restated in the form of a set of logical statements as follows:

Table 1 Discrete events and control actions[a]

Event	$s_R(k-1)$	$s_R(k)$	Inference	Control action
1	(0,0,0,0)	(0,0,0,0)	No sensor hit	Go to Coarse Mode
2	(0,0,0,0)	(1,0,0,0)	Beam enters LS	Right 1 step
3	(0,0,0,0)	(0,1,0,0)	L-R, TS hit, Hi-V	Left 1 step
4	(0,0,0,0)	(0,0,1,0)	R-L, RS3 hit, Hi-V	Left 1 step
5	(0,0,0,0)	(0,0,0,1)	Beam enters RS	Left 1 step
6	(1,0,0,0)	(0,0,0,0)	Beam exits LS	Right 1 step
7	(1,0,0,0)	(1,0,0,0)	B-S, RS1 hit	Right 1 step
8	(1,0,0,0)	(0,1,0,0)	TS hit	No step
9	(1,0,0,0)	(0,0,1,0)	L-R, RS3 hit, Hi-V	Left 2 steps
10	(1,0,0,0)	(0,0,0,1)	L-R, RS4 hit, ABN	Left 2 steps
11	(0,1,0,0)	(0,0,0,0)	Beam exits LS, Hi-V	Right 2 steps
12	(0,1,0,0)	(1,0,0,0)	R-L, RS1 hit	Right 1 step
13	(0,1,0,0)	(0,1,0,0)	B-S, TS hit	No step
14	(0,1,0,0)	(0,0,1,0)	L-R, RS3 hit	Left 1 step
15	(0,1,0,0)	(0,0,0,1)	L-R, RS4 hit,Hi-V	Left 2 steps
16	(0,0,1,0)	(0,0,0,0)	L-R, Hi-V, Beam exits RS	Left 2 steps
17	(0,0,1,0)	(1,0,0,0)	R-L, RS1 hit, Hi-V	Right 2 steps
18	(0,0,1,0)	(0,1,0,0)	R-L, TS hit	No step
19	(0,0,1,0)	(0,0,1,0)	B-S, RS3 hit	Left 1 step
20	(0,0,1,0)	(0,0,0,1)	L-R, RS4 hit	Left 1 step
21	(0,0,0,1)	(0,0,0,0)	Beam exits RS	Left 1 step
22	(0,0,0,1)	(1,0,0,0)	R-L, RS1 hit, ABN	Right 2 steps
23	(0,0,0,1)	(0,1,0,0)	R-L, TS hit, Hi-V	Right 2 steps
24	(0,0,0,1)	(0,0,1,0)	R-L, RS3 hit	Left 1 step
25	(0,0,0,1)	(0,0,0,1)	B-S, RS4 hit	Left 1 step

[a]RSi, ith sensor in right sensor array; TS, RS2 or target sensor; Hi-V, high angular speed regime; ABN, abnormal motion; L-R, beam moves from left to right; R-L, beam moves from right to left; B-S, beam stationary; LS, RS, left and right sides of sensor array, respectively.

if $s_R(k) = (1, 0, 0, 0)$ and $s_R(k-1) = (0, 0, 1, 0)$ or $(0, 0, 0, 1)$,
  then Right 2 steps;
  else Right 1 step;
if $s_R(k) = (0, 1, 0, 0)$, then
  if $s_R(k-1) = (0, 0, 0, 1)$, then Right 2 steps;
  if $s_R(k-1) = (0, 0, 0, 0)$, then Left 1 step;
  else No step;
if $s_R(k) = (0, 0, 1, 0)$, then
  if $s_R(k-1) = (1, 0, 0, 0)$, then Left 2 steps;
  else Left 1 step;
if $s_R(k) = (0, 0, 0, 1)$ and $s_R(k-1) = (1, 0, 0, 0)$ or $(0, 1, 0, 0)$,
  then Left 2 steps;
  else Left 1 step;
if $s_R(k) = (0, 0, 0, 0)$, then
  if $s_R(k-1) = (1, 0, 0, 0)$ then Right 1 step;
  if $s_R(k-1) = (0, 1, 0, 0)$ then Right 2 steps;
  if $s_R(k-1) = (0, 0, 1, 0)$ then Left 2 steps;
  if $s_R(k-1) = (0, 0, 0, 1)$ then Left 1 step;
  if $s_R(k-1) = (0, 0, 0, 0)$, then GOTO coarse mode.

From Table 1, it is clear that we have coarse control mode activation for event 1; intermediate control mode activation for events 6, 11, 16, and 21; and fine control mode activation for the remaining events. In our present experimental setup, the mirror servos are used in all control modes. Evidently, the combined system composed of Eq. (2), mirror servo, and the combiner sensor array, along with the foregoing control rules, can be regarded as a hybrid continuous-time and discrete-event system.

Experimental Results

The main objective of our experiment is to determine the effectiveness of the proposed rule-based cooperative controls for laser-beam acquisition and tracking in the presence of small-attitude drift. At the start of an experimental run, the magnetic levitation systems were activated. The MS were carefully balanced statically so that their rotational drift due to asymmetric mass distribution was minimized. The angles of the collector mirrors were offset from their desired values so that the reflected laser beams from the mirrors did not intercept the sensor array of the combiner. Because the moment of inertia of the mirror servo about the vertical rotational axis is small compared to that of the MS body, and the angular speed of the servo is small, there is negligible angular momentum transfer from the servo to the MS body.

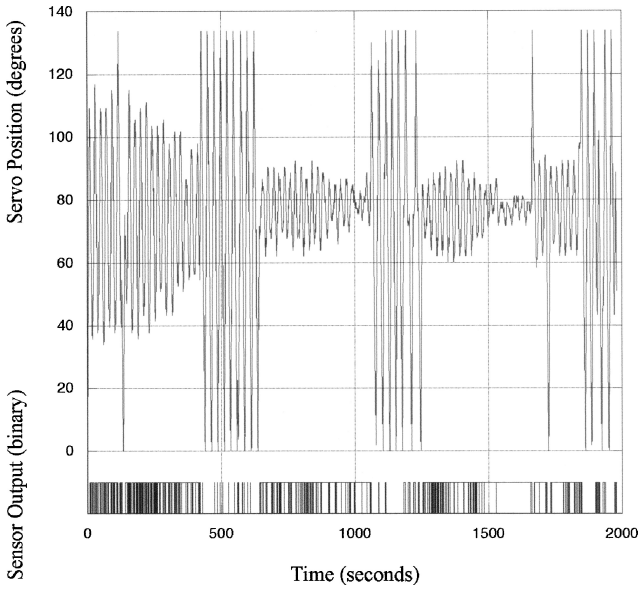

Fig. 8 Time history of mirror-servo motion and target-sensor output for left collector.

Figure 8 shows the mirror-servo motion and the output of the target sensor of the left collector for a 2,000-s run. The period where the target-sensor output is unity corresponds to laser-beam alignment. At the start of the experiment, the laser beam was on the target sensor. Because of slight nonuniformity in the magnetic fields of the electromagnets of the levitation systems, both the collector and the combiner oscillated about their vertical axes with a frequency about 0.01 Hz. Consequently, the mirror servo had to move in order to keep the laser beam on target as shown in the top record of Fig. 8. Because the sensor array has only four sensor elements, its resolution is limited to the width of a sensor element. No control

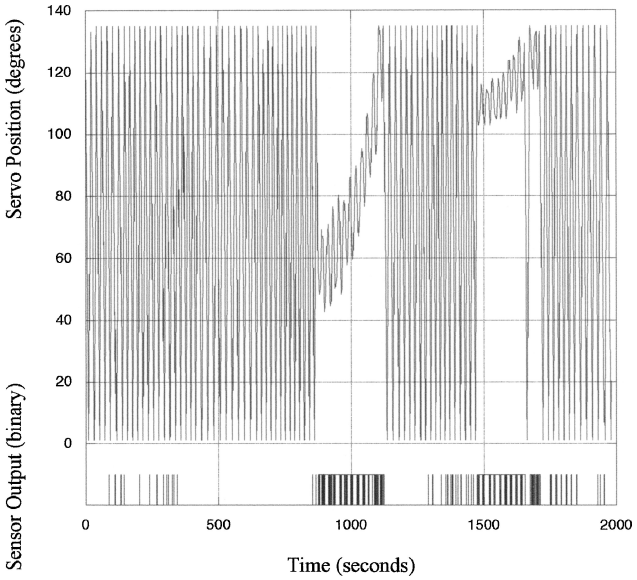

Fig. 9 Time history of mirror-servo motion and target-sensor output for right collector.

action is taken as long as the target sensor is activated by the laser beam. Control action is taken when the laser beam moves to another sensor element. It can be seen from the mirror-servo position record during the initial 420-s period that the servo had to move to keep the laser beam on the target sensor. The apparent chattering of the sensor output data during this period was due to the fact that the binary sensor output was obtained by feeding the analog sensor output through a threshold device (an analog comparator). Because the analog sensor output depended on the sensor-element area that was exposed to the laser beam, a small shift of the beam (about one-third the width of the sensor element) about the element center gave a zero binary output. To determine the performance of the rule-based controls for laser-beam acquisition, the laser beam was blocked manually between times $t = 420$ and 440 s. This caused the control to switch to the intermediate mode for recapturing the laser beam. Between times $t = 440$ and 610 s, the mirror servo moved back and forth between its minimum and maximum positions until the beam was recaptured at $t = 610$ s. The beam remained on target until $t = 1070$ s when the laser beam was blocked again manually. The beam was recaptured at $t = 1250$ s and remained on target until $t = 1700$ s.

Similar results for the right collector are shown in Fig. 9. Here the laser beam was initially off the target sensor implying that the right-collector control started in the coarse mode. Thus, the mirror servo of the right collector moved back and forth between its limiting positions until the target sensor was hit by the laser beam at $t = 860$ s. During this experimental run, the right-collector motion was composed of an oscillatory motion and a slow drift in one direction. The mirror servo on this collector had to move to compensate for this combined motion during the period $860 < t < 1140$ s, as shown in Fig. 9. At $t = 1140$ s, the slow drift resulted in a position beyond the range of the mirror servo. At this point the laser beam lost contact with the target sensor. A search for the laser beam was initiated again at this time. This scenario was repeated during the period $1480 < t < 1660$ s. Note that the motions of the right and left collectors were completely independent of each other. A video depicting the experimental setup and aforementioned experiments is available from the first author.

Discussion

In the design of the control rules, we have assumed that the combiner is stationary with respect to the laboratory inertial frame. When the combiner is nonstationary, it is necessary to have complete knowledge of the combiner motion so that correct inferences of the laser-beam motion relative to the combiner can be made. The proposed control rules can then be modified accordingly. In our combiner, neither velocity sensors nor precision positioning sensors comparable to star trackers in real spacecraft were installed.

In our rule-based control systems, the most undesirable mode switching occurs when a large disturbance causes the laser beam to walk off the target sensor after having been there long enough to switch to the fine mode. The control rule calls for rotation of the mirror in the direction of the last laser-beam/sensor contact. If the disturbance is sufficiently large, this search in the intermediate mode could fail and result in switching to the coarse mode.

Because the MS in our experimental setup do not have sensors that detect their own angular positions, the collector cannot differentiate between the laser pointing errors caused by its own rotation and that due to the combiner rotation when both levitated MS are subjected to disturbances. Thus, the mirror servo cannot be commanded to counteract the collector's own rotation. In the worst-case scenario where the combiner and collector rotate in opposite directions, the magnitude of the rotational laser pointing error is doubled from that for the case when one of them is stationary or when the combiner's rotational motion is known.

In our MS, a detrimental factor is due to the nature of the mirror servo, which responds to an input command and then holds to the corresponding angular position. The response time cannot be controlled by the user. Moreover, issuing a command to the servo while it is reacting to an earlier command gives unpredictable results. Thus, the overall performance is limited by the response time of the mirror command.

In spite of the aforementioned drawbacks and the small number of elements in the optical sensor array, it was found that the proposed cooperative control rules were effective as long as the combiner's angular speed remained sufficiently small over the time duration of the experiment.

Finally, in our experimental setup, only low-cost components are used. Therefore, we do not expect to achieve the system-performance specifications for a real space interferometer. Nevertheless, this experiment provides some insight into the effectiveness of a relatively simple multimode, rule-based controller for optical alignment, and the inherent difficulties in controlling the attitude of real free-flying spacecraft for interferometry in the presence of disturbances.

Conclusions

Our present experiment involves optical alignment of three MS, each with only one degree of freedom. However, the mirror platform in the collector MS is articulated, such as a robot arm with rotary joints. It is possible to modify our experimental setup to allow small vertical translational motion and also planar translational motion by attaching the present system to an air-levitated platform, such as that in our previous setup.[9] In this study, no attempt is made to include the effects of orbital and large translational motions of the spacecraft on the control system performance. The modification of our present MS to increase the rotational degrees of freedom under magnetic levitation is an extremely difficult task. The present setup is being modified for experiments involving acquisition of interference patterns produced by out-of-phase light beams. The results will be presented in the near future.

Acknowledgment

This work was performed under contract no. 960570 with the Jet Propulsion Laboratory, California Institute of Technology, Pasadena, California. The authors thank the referees for their helpful comments and suggestions.

References

[1]Fanson, J. L., Anderson, E. H., Moore, D. M., and Ealey, M. A., "Development of an Active Truss Element for Control of Precision Structures," *Optical Engineering*, Vol. 29, No. 11, 1990, pp. 1333–1341.

[2]Neat, G. W., Sword, L. F., Hines, B. E., and Calvet, R. J., "Micro-Precision Interferometer Test-Bed: End-to-End System Integration of Control Structure Interaction Technologies," *Proceedings of SPIE, Spaceborne Interferometry*, edited by R. D. Reasenberg, Vol. 1947, Society of Photo-Optical Instrumentation Engineers, Bellingham, WA, 1993, pp. 91–103.

[3]Melody, J. W., and Neat, G. W., "Integrated Modeling Methodology Validation Using the Micro-Precision Interferometer Testbed," *Proceedings of the 35th IEEE Conference on Decision and Control*, Vol. 4, IEEE Press, New York, 1996, pp. 4222–4227.

[4]Stannik, R. V., Melroy, P., McCormack, E. F., Arnold, D., and Gezari, D. Y., "Multiple Spacecraft Michelson Stellar Interferometry," *Proceedings of SPIE, Instrumentation in Astronomy V*, Vol. 445, Society of Photo-Optical Instrumentation Engineers, Bellingham, WA, 1984, pp. 358–369.

[5]DeCue, A. B., "Orbital Station-Keeping for Multiple Spacecraft Interferometry," *Journal of Astronautical Sciences*, Vol. 39, No. 3, 1991, pp. 283–297.

[6]Lau, K., Colavita, M., and Shao, M., "The New Millennium Separated Spacecraft Interferometer," *Space Technology and Applications International Forum*, edited by M. S. El-Gent, American Inst. of Physics, College Park, MD, 1997, pp. 245–250.

[7]Robertson, A., Corazzini, T., and How, J. P., "Formation Sensing and Control Technologies for a Separated Spacecraft Interferometer," *Proceedings of the American Control Conference*, Vol. 3, American Automatic Control Council, Evanston, IL, 1998, pp. 1574–1579.

[8]Tolker-Nielsen, T., and Oppenhaeuser, G., "In Orbit Test Results of an Operational Optical Intersatellite Link Between ARTEMIS and SPOT4, SILEX," *Proceedings of SPIE, Free-Space Laser Communication Technologies XIV*, edited by G. Stephen Mecherle, Vol. 4635, 2002, pp. 1–15.

[9]Wang, P. K. C., Yee, J., Hadaegh, F. Y., and Lau, K., "Experimental Study of Formation Alignment of Multiple Autonomous Air-Levitated Vehicles with Rule-Based Controls," *Journal of Robotic Systems*, Vol. 15, No. 10, 1998, pp. 559–580.

[10]Wang, P. K. C., Yee, J., and Hadaegh, F. Y., "Synchronized Rotation of Multiple Autonomous Model Spacecraft with Rule-Based Controls: Experimental Study," *Journal of Guidance, Control, and Dynamics*, Vol. 24, No. 2, 2001, pp. 352–359.